ACS APPLIED MATERIALS & INTERFACES

Research Article

www.acsami.org

Enzyme-Free Amplification by Nano Sticky Balls for Visual Detection of ssDNA/RNA Oligonucleotides

Shan Chen,[†] Lok Ting Chu,[†] Pak Piu Yeung,[†] Zichen Zhao,[†] Yuanye Bao,[†] Miu Shan Chan,[‡] Pik Kwan Lo,[‡] and Ting-Hsuan Chen*[,†,§,∥]

[†]Department of Mechanical and Biomedical Engineering, [‡]Department of Biology and Chemistry, [§]School of Creative Media, and [∥]Centre for Robotics and Automation, City University of Hong Kong, Hong Kong Special Administrative Region, China

Supporting Information

ABSTRACT: Visual detection of nucleic acids provides simple and rapid screening for infectious diseases or environmental pathogens. However, sensitivity is the current bottleneck, which may require enzymatic amplification for targets in low abundance and make them incompatible with detection at resource-limited sites. Here we report an enzyme-free amplification that provides a sensitive visual detection of ssDNA/RNA oligonucleotides on the basis of nano "sticky balls". When target oligonucleotides are present, magnetic microparticles (MMPs) and gold nanoparticles (AuNPs) were linked together, allowing the collection of AuNPs after magnetic attraction. Subsequently, the collected AuNPs, which carry many oligonucleotides, were used as the sticky balls to link a second pair of MMPs and polymer microparticles (PMPs). Thus, because the magnetic field can attract the MMPs as well as the linked PMPs to the sidewall, the reduction of suspended PMPs yields a change of light transmission visible by the naked eye. Our results demonstrate that the limit of detection is 10 amol for ssDNAs (228 fM in 45 μL) and 75 amol for ssRNAs (1.67 pM in 45 μL). This method is also compatible with the serum environment and detection of a microRNA, miR-155, derived from human breast cancer cells. With significantly improved sensitivity for visual detection, it provides great potential for point-of-care applications at resource-limited sites.

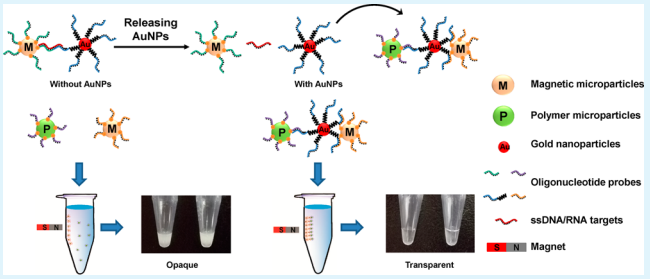

KEYWORDS: *nucleic acids, gold nanoparticles, microRNAs, visual detection, magnetophoretic effect*

1. INTRODUCTION

Visual detection of nucleic acids provides simple and rapid assays with visualized readout,[1] and has been widely used for pathogen identification[2−5] or disease diagnosis.[6−8] Nanomaterials, such as gold nanoparticles (AuNPs),[9−14] silver nanoparticles,[15] and graphene oxide,[16] have been employed for visual detection according to their unique optical properties, biocompatibility, conductivity, and high surface-to-volume ratio.[17−22] For example, AuNPs were used for detection of target molecules by modifying capturing probes on the surface of AuNPs.[14,17,23−25] As such, the presence of target molecules would cause the aggregation of AuNPs and induce a change of solution color from red to purple. Moreover, this scheme was recently developed into lateral flow strips and magnetophoretic assays that provide fast visual readout for detection of ssDNA/RNA oligonucleotides.[26−29] However, although promise was shown, these visual detections are subject to the limit of detection (LOD), which usually falls into nanomole per liter level because a large amount of target oligonucleotides is required to induce AuNP aggregation. Thus, without amplification, these methods are not desirable for detecting targets in low abundance.[30]

To improve the sensitivity of visual detection, various amplification methods have been suggested. Enzymatic amplification has been widely used in visual or other types of detection.[31−33] However, enzymatic amplifications require specific conditions for enzymatic reactions, e.g., thermal cycles, and special storage for protein enzymes that may be difficult for resource-limited sites. Therefore, enzyme-free amplification has attracted increasing attention, including biobarcode-based detection[34−36] or hybridization DNA circuits.[37−42] Biobarcode amplification uses target molecules to connect nanoparticles that carry a vast number of barcode DNAs. The barcode DNAs, whose amount is proportional to the target molecules, are subsequently dissociated from the nanoparticles and detected, resulting in amplified signals representing the target molecules. However, the dissociation of biobarcode DNAs may require time-consuming dithiothreitol (DTT) treatment[43] or toxic cyanide,[36] which may increase complexity of the assays. Alternatively, hybridization DNA circuits rely on short DNA strands that act as catalysts or triggers to initiate a series of opening and assembly of DNA hairpins;[37−42] therefore, an isothermal and enzyme-free amplification were achieved. However, possibly because of the undesired opening of hairpins, the sensitivity of these assays reached 10 fmol[37] or

Received: June 7, 2015
Accepted: October 2, 2015
Published: October 2, 2015

ACS Publications © 2015 American Chemical Society

DOI: 10.1021/acsami.5b05018
ACS Appl. Mater. Interfaces 2015, 7, 22821−22830

14−50 pM,[38,40,42] which requires improvement for point-of-care applications in practical aspects.

Here we report an enzyme-free amplification based on a new scheme: a nano "sticky balls" amplified magnetophoretic effect for sensitive and quantitative visual detection of ssDNA/RNA oligonucleotides (Scheme 1). Our method consists of two

Scheme 1. Working Principle of the Enzyme-Free Amplified Magnetophoretic Effect Using AuNPs as Nano Sticky Balls for Visual Detection of ssDNA/RNA Oligonucleotides

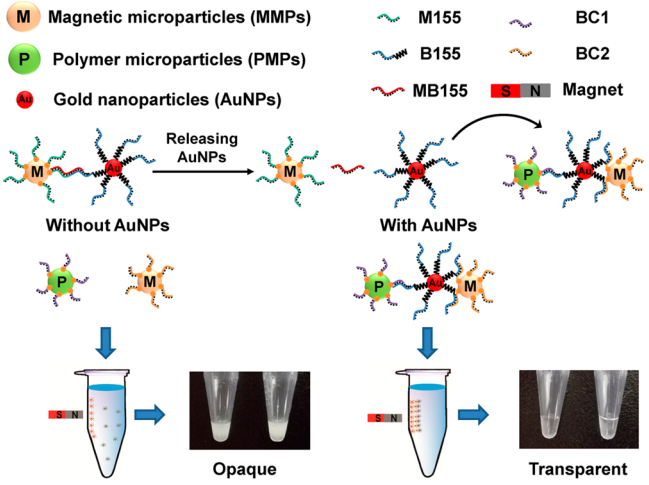

steps. In the first step, the AuNPs and magnetic microparticles (MMPs) were modified with oligonucleotide probes such that they can bind together by hybridizing with target oligonucleotides in juxtaposition which allows the collection of linked AuNPs via magnetic attraction. In the second step, the collected AuNPs were used as nano sticky balls connecting a second pair of MMPs and polymer microparticles (PMPs), forming a MMPs−AuNPs−PMPs complex. Therefore, after applying the magnetic field, the MMPs−AuNPs−PMPs could be moved to the sidewall, yielding a change of solution turbidity from opaque to transparent due to the reduction of suspended PMPs. Note that because the PMPs are large (1.04 μm in diameter) the change of turbidity is caused by Mie scattering that can effectively attenuate light transmission with significantly enhanced extinction coefficient (~3 orders of magnitude greater than that of commonly used gold nanoparticles[44]). More importantly, because the AuNPs are nanoscale, only very small amount of target oligonucleotides was required for the collection of AuNPs in the first step. Therefore, the few target nucleotides were exchanged to AuNPs modified with many oligonucleotide probes, which were used for the connection between MMPs and PMPs with significantly enhanced binding strength that amplified the signals. Using this enzyme-free amplification, we found that the LOD reached 10 amol for ssDNAs (228 fM in 45 μL) and 75 amol for ssRNAs (1.67 pM in 45 μL). Moreover, this method can be applicable for detection of the target oligonucleotides in the blood serum and microRNAs, miR-155, extracted from human mammary gland metastatic epithelial cells (MDA-MB-231 cell line). With greatly improved sensitivity, our approach shows potential for disease diagnosis with quantitative readouts at resource-limited sites.

2. EXPERIMENTAL SECTION

Materials and Reagents. The single-strand oligonucleotides, tris (2-carboxyethyl) phosphine (TCEP), and sodium dodecyl sulfate (SDS) were purchased from Sangon Biotech Ltd. The tris-ethyl-enediaminetetraacetic acid (Tris-EDTA) buffer, potassium phosphate, Tris-HCl, EDTA, Trition X-100, and NaCl were obtained from Sigma-Aldrich. The blood serum was fetal bovine serum from Life Technology. The MMPs of 0.90 μm in diameter (CM01N, Bangs Laboratories, Inc., USA) and PMPs of 1.04 μm in diameter (polystyrene basis, CP01F, Bangs Laboratories, Inc., USA) were functionalized with a streptavidin coating by the manufacturer using covalent conjugation with a zero-length cross-linker. The AuNPs with diameter of 30 nm were from PERSer Nanotechnology, Ltd. All chemicals were of analytical grade. Deionized (DI) water with a resistivity of 18.2 MΩ cm was obtained from a Milli-Q Plus system.

Oligonucleotide Sequence. The single-strand oligonucleotides were dissolved in Tris-EDTA buffer. These sequences are listed in Table 1. The oligonucleotide probes M155 and B155 were designed

Table 1. Sequences of the Oligonucleotides

strand name	sequence
M155[a]	5′-/biotin/-CCCCTATCACG-3′
B155[a]	5′-ATTAGCATTAAACTCGGATCACTCG-$(PEG)_6$- thiol-3′
Bi155[a]	5′-ATTAGCATTAA-/biotin/-3′
MB155	5′-TTAATGCTAATCGTGATAGGGG-3′
MBr155	5′-UUAAUGCUAAUCGUGAUAGGGG-3′
SNP A	5′-TTAAT***A***CTAATCGTGATAGGGG-3′
SNP T	5′-TTAAT***T***CTAATCGTGATAGGGG-3′
SNP C	5′-TTAAT***C***CTAATCGTGATAGGGG-3′
BC1[b]	5′-GTTTAATGCTAAT-/biotin/-3′
BC2[b]	5′-/biotin/-CGAGTGATCCGA-3′

[a]The sequences complementary to MB155 or MBr155 in juxtaposition are underlined. [b]The sequences complementary to B155 in juxtaposition are underlined.

with sequence complementarity to the target oligonucleotide MB155 in juxtaposition, and oligonucleotide probes BC1 and BC2 were designed with sequence complementarity to the oligonucleotide B155 in juxtaposition. (Complementary sequences are underlined.) The oligonucleotide B155 was functionalized with $(PEG)_6$-thiol at its 3′ end, which avoids steric hindrance during hybridization between BC2 and B155. Bi155 was designed on the basis of B155, but the $(PEG)_6$-thiol at its 3′ end was replaced by biotin. MBr155 is the RNA-based oligonucleotide designed accordingly to the sequence of MB155. SNP A, SNP T, and SNP C were designed with a single-base mismatch (shown in bold italic) compared to MB155.

Modification of AuNPs. $(PEG)_6$-thiol-functionalized probe B155 (100 μM, 25 μL) was first activated by 5 equiv of TCEP for 1 h. Then, the TCEP-activated B155 was added to 1 mL of gold nanoparticles (30 nm, 300 pM) at room temperature. After 16 h, 0.01% SDS was added to the solution, and it was brought to a final concentration of 1.0 M NaCl through a stepwise process. Upon aging for 40 h, the AuNPs were isolated by centrifugation 13.8 × g for 10 min, washed three times with hybridization buffer (pH 7.4, 10 mM phosphate, 0.3 M NaCl, 0.01% SDS), dispersed in the hybridization buffer, and finally stored at 4 °C until use. To estimate the number of oligonucleotides loaded on the AuNPs, we used FAM-labeled DNAs to modify AuNPs. The FAM-labeled DNAs were later dissociated by mixing with an equal volume of 1.0 M DTT in 0.18 M PBS buffer (pH 8.0) for incubation overnight.[43] After removing AuNPs by centrifugation, the fluorescence of the solution was measured and compared to a standard curve of the fluorescence intensity and FAM concentration. By this method, we found that there were approximately 330 oligonucleotides loaded on each AuNP, which was equal to $2.919 \times 10^{12}/cm^2$.

Modification of MMPs and PMPs. The oligonucleotide probes (M155, Bi155, BC1, and BC2) were biotinylated so that they can

DOI: 10.1021/acsami.5b05018
ACS Appl. Mater. Interfaces 2015, 7, 22821−22830

spontaneously attach to streptavidin-coated MMPs and PMPs. Briefly, 3.5 μL of MMPs or PMPs solution (10 mg/mL; 1.278×10^{10} and 1.617×10^{10} particles/mL for MMPs and PMPs, respectively) was added to the solution containing 2.5 μg of oligonucleotide probes. Note that each MMP and PMP would allow the attachment of 1.6×10^6 and 2.5×10^5 oligonucleotide probes, respectively (6.28×10^8 /cm^2 on MMPs and 4.32×10^8 /cm^2 on PMPs). Here, 2.5 μg of oligonucleotide probes were mixed with 35 μg of MMPs or PMPs, which is equal to 3.5×10^6 and 5.4×10^5 oligonucleotide probes for each MMP and PMP, respectively. Thus, the provided number of oligonucleotide probes is significantly greater than the total capacity of microparticles, which ensures that all binding sites were fully loaded. The mixture was incubated for 30 min at room temperature with gentle shaking to allow the immobilization of biotinylated oligonucleotides on streptavidin-coated microparticles. Next, the MMPs and PMPs were rinsed three times with 200 μL of wash buffer (20 mM Tris-HCl, pH 7.5, 1 M NaCl, 1 mM EDTA, 0.0005% Trition X-100) to remove residual oligonucleotides. For each washing step, the MMPs were collected using a magnetic separation rack, whereas the PMPs were collected using a centrifuge (13.8 × g for 5 min). At the end, the MMPs and PMPs were suspended in hybridization buffer with the final concentration 10 mg/mL.

Hybridization of MMPs and AuNPs with Target Oligonucleotides. For the detection of oligonucleotide, 1 μL of control sample containing pure hybridization buffer, target oligonucleotide solution with varying concentration prepared in hybridization buffer, or target oligonucleotides with single-base mismatch at 250 pM in hybridization buffer was added to 3.5 μL of MMPs (10 mg/mL) modified with M155 probes. For MBr155, RNAase inhibitor at 1 U/μL was supplemented. Hybridization was conducted for 30 min with gentle vortexing at room temperature. Then, 40.5 μL of B155-modified AuNPs was added to the mixed solution, hybridization was allowed with gentle vortexing for 30 min, and the final volume became 45 μL.

Hybridization of MMPs and AuNPs with Target Oligonucleotides in Blood Serum. Pure blood serum (1 μL of control sample) or blood serum containing varying concentration of target oligonucleotides MB155 was added to 3.5 μL of MMPs (10 mg/mL) modified with M155 and hybridization was allowed for 30 min with gentle vortexing at room temperature. Then, the MMPs with target oligonucleotides were collected by magnetic field. After rinsing the MMPs three times to remove the residue from blood serum, 4.5 μL of hybridization buffer was added. Next, 40.5 μL of B155-modified AuNPs were added allowed to hybridiz with gentle vortexing for 30 min, and the final volume was left as 45 μL.

Collection of Linked AuNPs. After hybridization, the MMPs−targets−AuNPs could be attracted to the sidewall by applying the magnetic field for 2 min, and the unlinked AuNPs were removed. Next, the MMPs−targets−AuNPs were resuspended in 5 μL of DI water and heated at 70 °C for 5 min to release the AuNPs. Note that the thiol−gold bond can remain stable in this heating step.[34,35] Finally, the salt concentration of the released-AuNPs solution was adjusted by adding 5 μL of 2× hybridization buffer (pH 7.4, 20 mM phosphate, 0.6 M NaCl, 0.02% SDS), and the final volume was 10 μL.

Visual Detection of MMPs−AuNPs−PMPs Based on Magnetophoretic Effect. To the solution of released AuNPs was then added 3.5 μL of BC2-modified MMPs (10 mg/ml), and hybridization was conducted with gentle vortexing at room temperature for 60 min. Next, to the mixture was added 3.5 μL of BC1-modified PMPs (10 mg/mL), and hybridization was conducted with gentle vortexing for 60 min at room temperature. The final volume was 17 μL. Finally, a magnetic field was applied for 2 min to attract the unreacted MMPs and MMPs−AuNPs−PMPs to the sidewall so that the solution with PMP suspension can be collected for direct visual inspection or quantitative analysis by UV−vis spectrometer (BioDrop μLITE, UK).

Cell Culture. MDA-MB-231 human mammary gland metastatic epithelial cells (ATCC, USA) were cultured in Dulbecco's modified Eagle's medium/nutrient mixture F-12 (DMEM/F-12) supplemented with 10% fetal bovine serum and 1% penicillin−streptomycin (PS). MCF-10A human mammary gland epithelial cells (ATCC, USA) were cultured in DMEM/F-12 supplemented with 5% horse serum (HS), 1% PS, 20 ng/mL epidermal growth factor, 0.5 mg/mL hydrocortisone, and 10 ug/mL insulin. For neutralizing the toxicity of trypsin during passaging, a resuspension medium for MCF-10A cells was prepared using DMEM/F-12 supplemented with 20% HS and 1% PS. All the cell lines were incubated at 37 °C in a humidified incubator (5% CO_2 and 95% air) and passaged every 3 days.

Extraction and Detection of MicroRNAs from Cells. Trizol (1 mL) was added to 6 million cells (or fewer) for 5 min at room temperature. Then, 0.2 mL of chloroform was added and vortexed for 15 s. The mixed solution was incubated on ice for 10 min and centrifuged at 13.8 × g at 4 °C for 15 min. Next, the upper aqueous phase was transferred to a new tube, and to this was added 0.5 mL of isopropyl alcohol with gentle vortexing, followed by incubation for 10 min. The mixed solution was centrifuged at 13.8 × g at 4 °C for 15 min, and the supernatant was removed. After adding 1 mL of ethanol to wash the RNAs gently, the mixture was centrifuged at 13.8 × g at 4 °C for 5 min, followed by removal of the supernatant and drying to make sure all the ethanol had been evaporated. Finally, DEPC-treated water was added, and the mixture was incubated at 65 °C to resuspend the RNAs in a final volume of 7 μL for storage at −80 °C. DEPC-treated water without RNA (7 μL) was used as the control sample. For detection, the RNA solution was added with PCR buffer (200 mM Tris HCl (pH 8.4), 500 mM KCl, 15 mM $MgCl_2$) to adjust salt concentration and RNAase inhibitor at 1 U/μL, and the final volume was adjusted to 10 μL. The RNA solution was then incubated with 3.5 μL of MMPs solution for 0.5 h, followed by isolation of MMPs and hybridization with AuNPs for subsequent visual detection via the aforementioned procedure.

Quantitative Reverse Transcription PCR (qRT-PCR). Total RNAs was extracted from 0.68 million cells (MDA-MB-231 and MCF-10A) using a commercial kit (12183555, Life Technology), and its concentration was measured via Biodrop (BioDrop μLITE, UK). The RNA solution from both cell types was mixed with reverse transcription (RT) master mix solution (4366596, Life Technology) and RT primer (assay no. 002623 for miR-155 or assay no. 001973 for U6, the endogenous normalizer, 4427975, Life Technologies). The sealed tube was incubated on ice for 5 min, followed by thermal cycles according to the kit protocol. After reverse transcription, the RT product was added to TaqMan Universal Master Mix II (4440038, Life Technology) and TaqMan Assay 20× (4427975, Life Technologies) following the kit protocol. The sealed strips were loaded into the real-time PCR system (Bio-Rad CFX Connect Real-Time System) following the kit protocol. All samples were repeated three times. The qRT-PCR results were analyzed by relative expression of miR-155 in fold changes by $\Delta\Delta C_T$ (cycle threshold) method.

3. RESULTS AND DISCUSSION

Nano Sticky Balls Amplified Magnetophoretic Effect. The working principle is illustrated in Scheme 1. For the target oligonucleotide MB155, we adopted a sequence the same as that of a type of microRNA, miR-155, that is highly expressed in breast cancer cells. This assay consists of two steps. In the first step, because oligonucleotide probes M155 and B155 were designed with sequence complementary to that of the target oligonucleotide MB155 in juxtaposition (Table 1), the MMPs modified with M155 and AuNPs modified with B155 were linked together via hybridization with target oligonucleotides MB155, forming MMPs−targets−AuNPs complex. After applying a magnetic field, the MMPs and MMPs−targets−AuNPs would be attracted to the sidewall. Note that in this step the solution color was unchanged because only small amount of AuNPs were attracted. After removing the unused AuNPs, the linked AuNPs were released by nucleic acid denaturation. In the second step, the released AuNPs containing hundreds of B155 oligonucleotides with sequence complementary to the sequence of BC1 and BC2 (Table 1) were acting as the sticky

DOI: 10.1021/acsami.5b05018
ACS Appl. Mater. Interfaces 2015, 7, 22821−22830

balls that can link BC2-modified MMPs and BC1-modified PMPs by hybridization in juxtaposition, forming a MMPs−AuNPs−PMPs complex. Thus, when a magnetic field was applied, the MMPs−AuNPs−PMPs were moved to the sidewall and induced a change of solution turbidity from opaque to transparent due to the reduction of PMPs in the solution (Movie S1). Note that the PMPs were chosen as the visual effectors in the magnetophoretic assay because of their large size, which allows an effective change of light transmission via Mie scattering.

We first optimized the ratio of MMPs and PMPs. Using 2.25 fmol (7.5 μL at 300 pM) or 0.45 fmol (1.5 μL at 300 pM) of AuNPs modified with B155 to link MMPs with BC2 and PMPs with BC1, the ratio of MMPs and PMPs was varied to obtain the greatest reduction of solution turbidity. By changing the PMP concentration while keeping the MMP concentration intact (35 μg in 17 μL), the most significant reduction of solution turbidity was achieved when the ratio of MMPs and PMPs is 1:1 (Figure S1). This condition was observed for both high and low concentrations of AuNPs. Alternatively, by changing the MMP concentration only, a similar result was obtained for a high concentration of AuNPs (Figure S2). Notably, the absorbance was slightly lower when the ratio is 1:0.5 or 1:0.25 if a low concentration of AuNPs was used. However, because this improvement was subtle and not applicable for a high concentration of AuNPs, the ratio of MMP and PMP was chosen as 1:1 for the optimized combination.

We next tested the feasibility of this AuNP-based amplification. As shown in the Figure 1, using target

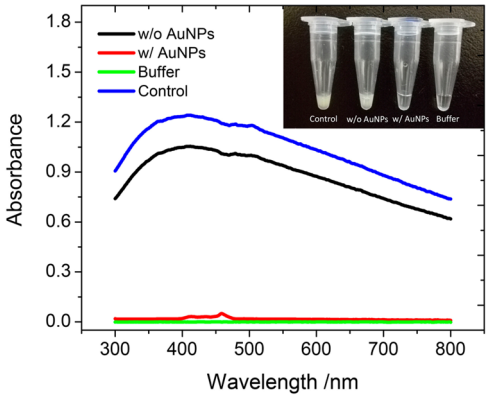

Figure 1. Spectral absorbance and (inset) optical images of the solution with PMP suspension resulting from the tests with or without AuNP amplification.

oligonucleotides at 250 pM in the first step, the AuNP-amplified magnetophoretic effect caused the solution turbidity to become as transparent as that of the buffer solution. Measured by UV−vis spectrometer, the spectral absorbance was almost the same (red and green lines in Figure 1). For comparison, we conducted another experiment where 1 nM B155 oligonucleotide molecules were directly applied to the mixture of BC2-modified MMPs and BC1-modified PMPs. Without AuNP amplification, the results showed that the solution was almost as opaque as the control sample that only had MMPs and PMPs. The UV−vis spectrum also showed that the absorbance only decreased little (black line in Figure 1) compared to that of control sample (blue line in Figure 1). Thus, using AuNPs as the nano sticky balls for signal amplification, the sensitivity was significantly enhanced.

Limit of Detection. We next explored the LOD of this method. As shown in Figure 2A, with the use of different concentrations of target oligonucleotide MB155 ranging from 1 pM to 250 pM, the solution turbidity gradually changed from opaque to transparent. Thus, the LOD was 2.25 fmol (50 pM in 45 μL) as determined by the naked eye. In addition, measured by spectral absorbance (Figure 2B,C), the calibration graph was linear in the range of 1−100 pM (Figure 2D), with calibration equation determined as $\lg(RA) = -0.00968C_{MB155} - 0.05498$, where RA is the relative absorbance at 400 nm, C_{MB155} is the concentration of MB155, and the corresponding correlation coefficient (R^2) of the calibration curve is 0.9474. On the basis of the calibration graph, the LOD was 10 amol (228 fM in 45 μL, calculated on the basis of $3\sigma/m$, where σ is the standard deviation of the $\lg(RA)$ of control sample, and m is the absolute slope of the calibration equation), which is much better than that of other types of visual assays such as AuNP aggregation with DNA circuit[38,40,42,45] or lateral flow strip.[26]

Notably, the target MB155 is a DNA oligonucleotide. Because short RNA oligonucleotides are extremely degradable, it may not be compatible with the operation principle and may be damaged during the detection procedure, even in well-defined buffer solution. To demonstrate the compatibility of RNAs, we used MBr155, which is an RNA-based oligonucleotide designed according to the sequence of target DNA MB155. Measured by spectral absorbance (Figure 2E), the calibration graph was linear in the range of 1−250 pM (Figure 2F). The calibration equation was determined as $\lg(RA) = -0.0017C_{MBr155} - 0.16673$, where RA is the relative absorbance at 400 nm, C_{MBr155} is the concentration of MBr155, and the corresponding correlation coefficient (R^2) of the calibration curve is 0.971. On the basis of the calibration graph, the LOD was 75 amol for ssRNAs (1.67 pM in 45 μL, calculated on the basis of $3\sigma/m$). The result showed that we can still achieve a low level of LOD, validating the compatibility and practicability of both DNA and RNA biomarkers in our amplified visual detection.

Amplification Rate. We next determined the amplification rate by comparing the signal with/without AuNP amplification. To conduct detection without AuNP amplification, we used two types of oligonucleotide probes, M155 and Bi155, with sequences complementary to that of the target oligonucleotide MB155 in juxtaposition. M155 and Bi155 were modified to MMPs and PMPs, respectively, and MMPs−targets−PMPs were formed after hybridization. The result showed that we can detect the concentration as low as 250 pM (Figure S3; relative absorbance, 0.94, total volume for hybridization, 45 μL). Compared to the detection with AuNP amplification, a similar readout was achieved for MB155 at 1 pM (Figure 2; relative absorbance, 0.91, total volume for hybridization, 45 μL). Thus, the amplification rate is about 250.

Selectivity of Single-Nucleotide Polymorphisms. We next investigated the selectivity of single-nucleotide polymorphisms, which is important for preventing nonspecific bindings and applications in gene expression assays. The seventh base G in MB155 was replaced by A, T, and C (SNP A, SNP T, and SNP C, respectively; Table 1). Using 250 pM in 45 μL, a concentration above the linear range, the results showed that although the solution turbidity become transparent for target molecules with complementary sequence the single-base-mismatched sequence caused the solution to remain opaque

DOI: 10.1021/acsami.5b05018
ACS Appl. Mater. Interfaces 2015, 7, 22821−22830

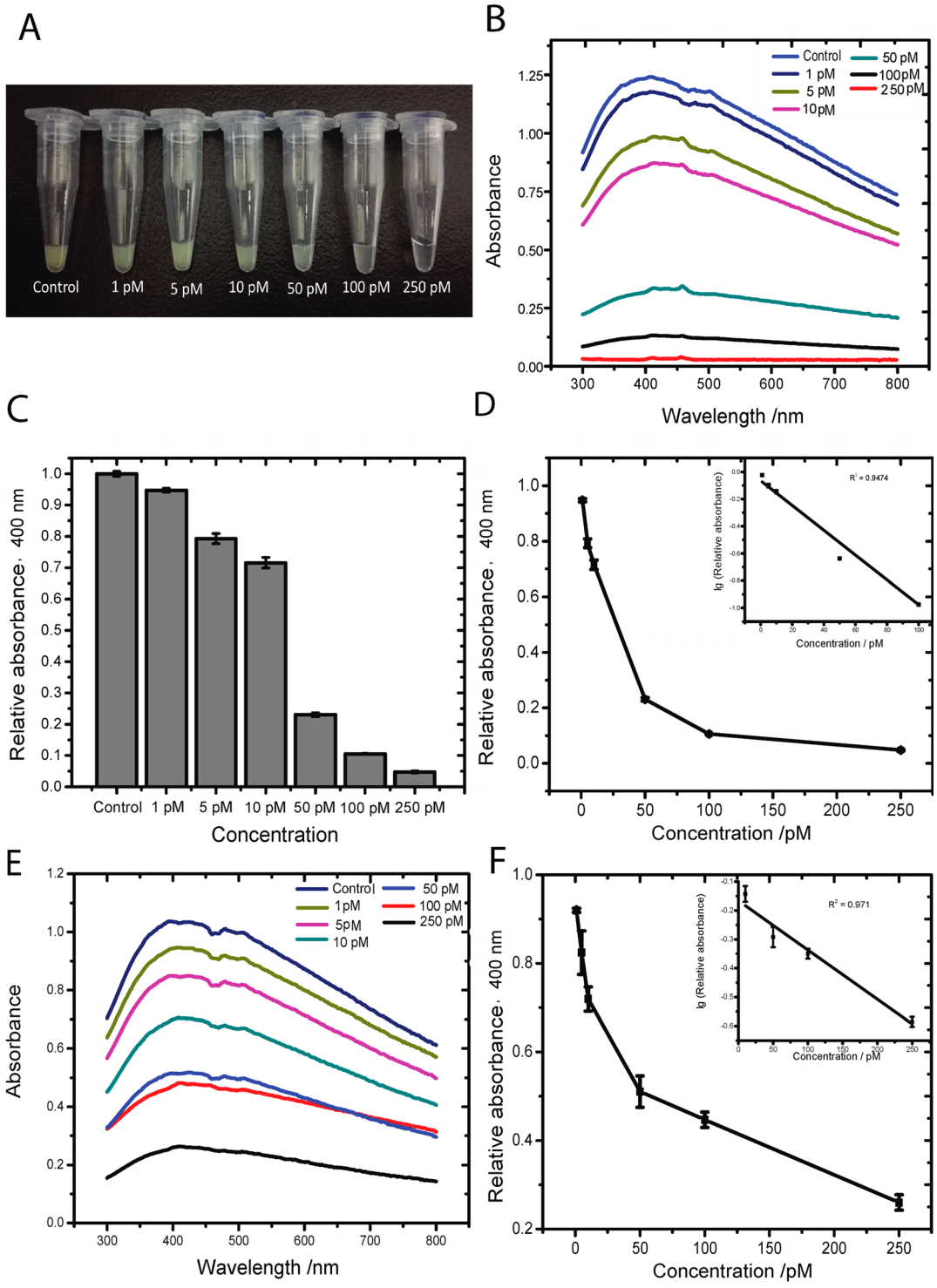

Figure 2. Visual detection of ssDNA/RNA oligonucleotides with varying concentrations (0 M, 1 pM, 5 pM, 10 pM, 50 pM, 100 pM, 250 pM in 45 μL). (A) Optical images showing the change of solution turbidity resulting from ssDNA MB155. (B) Spectral absorbance of the solution with PMP suspension resulting from ssDNA MB155. (C) Relative absorbance at 400 nm of data shown in B (mean ± max deviation, n = 3). Absorbance of the solution with PMP suspension resulting from the control sample was used as the reference. (D) Linear range of the relative absorbance with respect to the concentration of ssDNA MB155. (E) Spectral absorbance of the solution with PMP suspension resulting from ssRNA MBr155. (F) Linear range of the relative absorbance with respect to the concentration of ssRNA MBr155 (mean ± max deviation, n = 2).

(Figure 3A). In addition, as measured by UV−vis spectrometer, there was only a slight decrease of absorbance compared to that of the control sample (Figure 3B). The selectivity contrast ratio of SNP A, SNP T, and SNP C is 28, 30, and 36, respectively. Therefore, this result demonstrates the selectivity of our method for differentiating between target oligonucleotides with single-base-mismatched sequences.

Detection in Serum Environment. Some types of nucleic-acid-based biomarkers, such as microRNAs in blood-stream, were recently found to have promise for cancer

DOI: 10.1021/acsami.5b05018
ACS Appl. Mater. Interfaces 2015, 7, 22821−22830

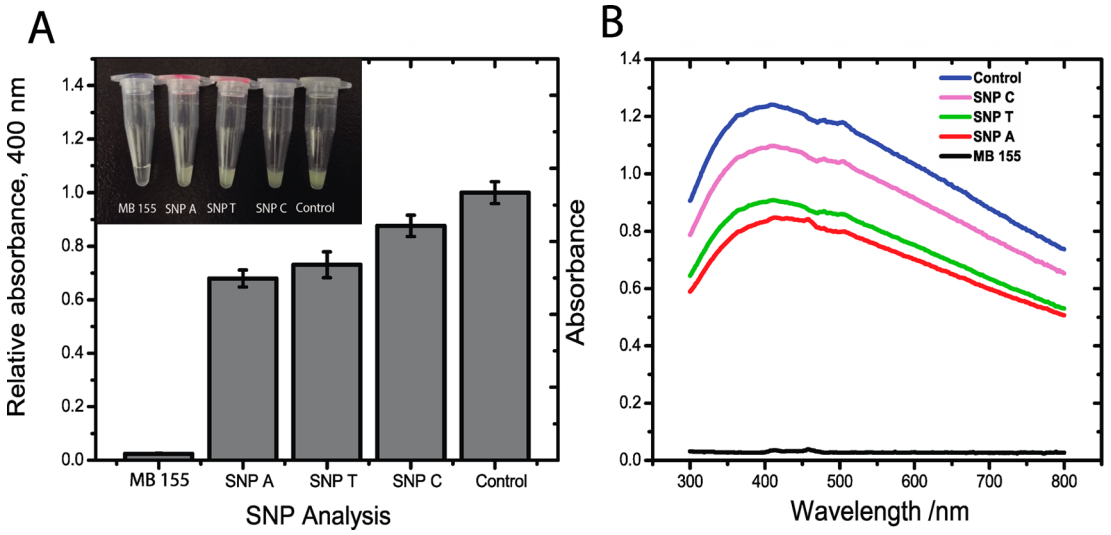

Figure 3. Detection of target oligonucleotides with single-base-mismatched sequence at 250 pM in 45 μL. (A) Optical images and relative absorbance at 400 nm of the solution with PMP suspension resulting from the control sample, solutions containing SNP A, SNP T, or SNP C with single-base-mismatched sequence, or solution containing MB155 with complementary sequence (mean ± max deviation, n = 3). Absorbance of the solution with PMP suspension resulting from the control sample was used as the reference. (B) Spectral absorbance of the solution with PMP suspension.

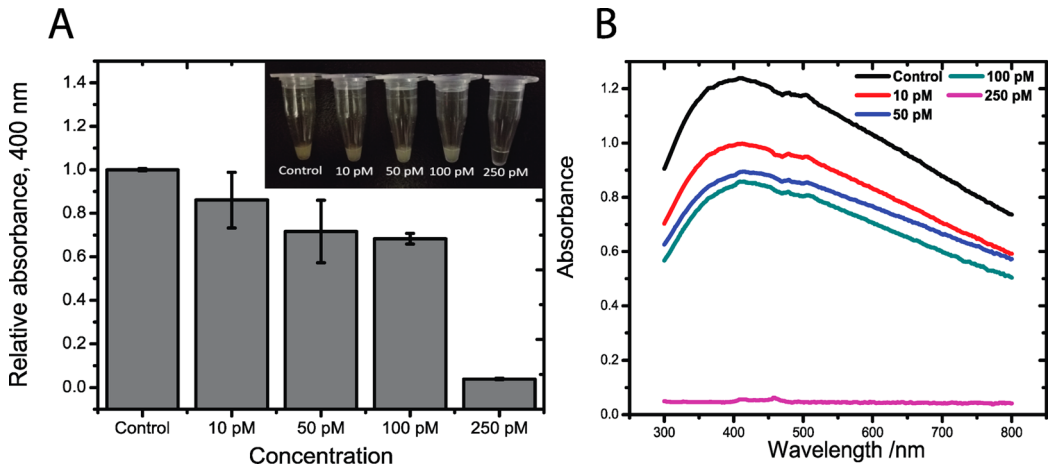

Figure 4. Detection of target oligonucleotides MB155 in blood serum. (A) Optical images and relative absorbance at 400 nm of solution with PMP suspension resulting from the control sample or solutions containing target oligonucleotides MB 155 with varying concentrations (0 M, 10 pM, 50 pM, 100 pM, 250 pM in 45 μL) (mean ± max deviation, n = 4). Absorbance of the solution with PMP suspension resulting from the control sample was used as the reference. (B) Spectral absorbance of the solution with PMP suspension.

classification and prognostication.[46] However, the presence in complex biofluid such as blood serum, which contains many interfering materials, e.g., protein, RNAs, DNase/RNase, may create considerable challenges or even complete failure of detection. To demonstrate the compatibility with complex biofluid, we next investigated the detection of target oligonucleotides MB155 with varying concentration in the blood serum. The results showed that the solution turbidity can still gradually changed from transparent to opaque with addition of target oligonucleotides (Figure 4) where the LOD was 100 pM in 45 μL by naked eyes and 2.7 pM in 45 μL by UV−vis spectra measurement (linear range, 0−100 pM, calculated on the basis of $3\sigma/m$) demonstrating the compatibility with complex biofluid.

Detection of RNAs Extracted from Cells. To further demonstrate the ability of detecting real biological markers, we applied this assay for detecting microRNAs derived from in vitro cell culture. The target oligonucleotide MB155 was designed with a sequence the same as a type of microRNA, miR-155, that is highly expressed in breast cancer cells (MDA-MB-231).[36] Thus, the oligonucleotide probes used above can be directly applied for detecting the miR-155 extracted from MDA-MB-231 cells. For comparison, the RNAs extracted from MCF-10A cells, the breast epithelial cell line, was also used as a reference.

We first investigated the expression level of miR-155 for both cell types. Using qRT-PCR, the results showed that the miR-155 was indeed highly expressed in MDA-MB-231 cells but not in MCF-10A cells (Figure 5A), which is consistent with previous findings.[47,48] After isolating the total RNAs from both cell types, the RNA solution was directly applied to our AuNP-amplified assay. The results showed a significant decrease of absorbance for RNA samples from MDA-MB-231 cells, suggesting that miR-155 was detected (Figure 5B,C). In

DOI: 10.1021/acsami.5b05018
ACS Appl. Mater. Interfaces 2015, 7, 22821−22830

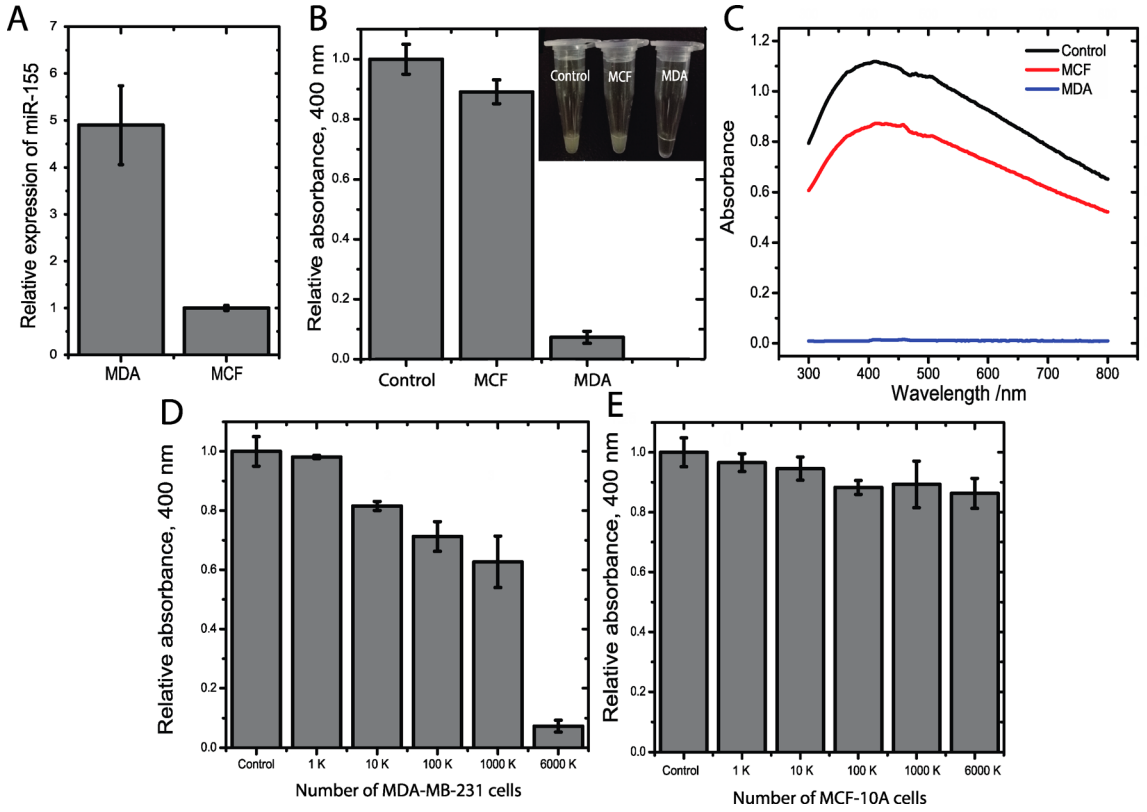

Figure 5. Detection of microRNA miR-155 extracted from MDA-MB-231 cells (MDA) or MCF-10A cells (MCF). (A) qRT-PCR analysis of the relative expression of miR-155 from MDA cells or MCF cells (mean ± SEM, n = 3). (B) Optical images and relative absorbance at 400 nm of the solution with PMP suspension resulting from the control sample or solutions containing extracted microRNAs (mean ± max deviation, n = 3). (C) Spectral absorbance of the solution with PMP suspension. (D and E) Relative absorbance at 400 nm of the solution with PMP suspension resulting from microRNAs extracted from varying number of MDA cells (D) or MCF cells (E) (mean ± max deviation, n = 3). Absorbance of the solution with PMP suspension resulting from the control sample was used as the reference.

contrast, for the MCF-10A cells, there was only a slight decrease of absorbance compared to the control sample, which may have resulted from the nonspecific adsorption of cellular components or low expression of miR-155 in cell lysates.

Furthermore, using different numbers of MDA-MB-231 cells for detection, the results showed a quantitative correlation between the absorbance and cell number, demonstrating the potential for quantitative analysis of our assays (Figure 5D). For MCF-10A cells, the decrease of absorbance remained at a similar level regardless of the increase of cell number (Figure 5E). Consequently, the result indicates that our method provides a potential solution for the detection of microRNAs and disease diagnosis with quantitative readouts.

4. DISCUSSION

In this paper, we demonstrate enzyme-free amplification via a Mie scattering based magnetophoretic assay for visual detection of ssDNA/RNA oligonucleotides. Magnetophoretic effect has been suggested as an effective approach for detection of ssDNA/RNA oligonucleotides.[28,29,37] On the basis of a colorimetric signal produced by AuNPs,[28,29] the LOD at 50[28] and 100 pM[29] was obtained. In addition, combining electrochemiluminescence signal and hybridization DNA circuits,[37] magnetophoretic effect was also employed for the detection of microRNAs, and the LOD was improved to 10 fmol. Compared to the aforementioned methods, our assay using Mie scattering with magnetophoretic assay, this nonenzymatic amplification demonstrated the LOD of 10 amol for ssDNAs (228 fM in 45 μL) and 75 amol for ssRNAs (1.67 pM in 45 μL), which is, to our knowledge, so far the most sensitive visual detection of ssDNA/RNA oligonucleotides. In addition, comparing total analysis time among different amplifications, our assay requires 3 h, which is comparable with the requirements of enzymatic methods (2 h and 40 min),[49] DNA circuits (4 h),[45] and biobarcode assay (3−4 h).[34] With similar total analysis time, this AuNP-based amplification does not require enzymatic reaction or additional chemical reaction to dissociate biobarcode oligonucleotides and is compatible with the blood serum or detection of microRNAs extracted from cell lysates.

Although our method is compatible with the serum environment, the interfering materials indeed caused decreased sensitivity and greater fluctuation of the readouts. As compared in the analytical figures of merit for detection in buffer solution or blood serum (Table 2), the assays in blood serum showed decreased sensitivity from 0.00968 to 0.00109 and increased LOD from 228 fM to 2.7 pM (total volume, 45 μL). More importantly, the increased fluctuation can be observed and quantified by the increase of relative standard deviation (RSD). This reduction of detection performance may be partially due

Table 2. Comparison of the Analytical Figures of Merit

	in buffer	in serum
sensitivity (pM^{-1})	0.00968	0.00109
LOD (pM)	0.228	2.7
RSD (%)	1.1 (10 pM)	8.5 (10 pM)

DOI: 10.1021/acsami.5b05018
ACS Appl. Mater. Interfaces 2015, 7, 22821−22830

to nonspecific bindings of proteins present in blood serum, causing particle agglomeration or making the particles dispersion unstable. Moreover, the presence of DNase/RNase may also provide a negative influence on the detection efficacy. Because MMPs were used to capture the target oligonucleotide, surface modification with blocking agents may be needed to obtain the same level of sensitivity conducted in the buffer solution.

Notably, PMPs of 1.04 μm in diameter were used as the visual effectors, which provide a significantly enhanced extinction coefficient due to the Mie scattering. Mie scattering describes a phenomenon where an electromagnetic plane wave passes by homogeneous spheres, of which the size is comparable to or greater than the wavelength of light.[44,50−54] Using dynamic light scattering, the results showed that the diameter of PMPs is 1.1 ± 0.23 μm (mean ± standard deviation) (Figure S4), which does not significantly deviate from the manufacturer's specification and meets the requirement of Mie scattering. We calculated the extinction coefficient according to the Lambert−Beer Law, $A_\lambda = \varepsilon cL$, where A_λ is the spectral absorbance at the wavelength of λ = 400 nm, ε is extinction coefficient, and L is the path length of light, 0.05 cm. The concentration c of the stock solution of PMPs was calculated on the basis of the number concentration provided by the manufacturer (1.617×10^{10} particles/mL, which is equal to 2.686×10^{-11} M). On the basis of the measured absorbance for a serial dilution of PMP suspension, the extinction coefficient ε was calculated as 4.457×10^{12} M^{-1} cm^{-1}. Compared to AuNPs, which are commonly used in many types of visual detection and have an extinction coefficient at the scale of 10^9 M^{-1} cm^{-1} for a diameter of 20−40 nm,[55] the extinction coefficient of PMPs using Mie scattering is 3 orders of magnitude greater. Thus, the improved sensitivity in our visual method can be attributed to the significantly enhanced binding strength of nano sticky balls as well as the increased extinction coefficient by Mie scattering.

5. CONCLUSIONS

Visual detection is a powerful method for detection at resource-limited sites because of its simple and instrument-free procedure. However, the current bottleneck is sensitivity that usually falls at a nanomoles per liter level and is insufficient for detecting target molecules in low abundance. Using AuNPs as nano sticky balls to amplify the magnetophoretic effect in an enzyme-free manner, we report an improved LOD of 10 amol for ssDNAs (228 fM in 45 μL) and 75 amol for ssRNAs (1.67 pM in 45 μL). Compared to other amplification methods such as enzymatic amplifications that require incubation with specific conditions for enzymatic reaction, biobarcode-based amplification that requires additional chemical reaction to dissociate oligonucleotides from AuNPs, which is nontrivial, and hybridization chain reaction that may be subject to undesired hairpin opening even when target is absent, our method only needs two steps, and the whole procedure could be finished with low requirement of facilities (mostly by pipettes and a magnetic rack), which allows simple and direct assays for point-of-care applications. More importantly, we have also demonstrated its ability for detecting target oligonucleotides in blood serum or microRNAs extracted from the breast cancer cells. Therefore, we show a simple and highly sensitive visual method that has a potential application for wide range of applications such as on-site examination in the future.

■ ASSOCIATED CONTENT

Supporting Information

The Supporting Information is available free of charge on the ACS Publications website at DOI: 10.1021/acsami.5b05018.

Optimization of the MMPs:PMPs ratio by varying the PMP concentration, optimization of the MMPs:PMPs ratio by varying the MMP concentration, detection without AuNP amplification, and the size distribution of PMPs. (PDF)

A movie illustrating the change of solution turbidity from opaque to transparent due to the reduction of suspended PMPs after applying a magnetic field. (MPG)

■ AUTHOR INFORMATION

Corresponding Author

*E-mail: thchen@cityu.edu.hk. Fax: (+852) 3442 0172. Telephone: (+852) 3442 4114.

Notes

The authors declare no competing financial interest.

■ ACKNOWLEDGMENTS

We are pleased to acknowledge support from the National Natural Science Foundation of China (grant no. 51305375), an Applied Research Grant (grant no. 9667097) and an Idea Incubator Scheme (grant no. 6987032) from City University of Hong Kong, and the Early Career Scheme of Hong Kong Research Grant Council (project no. 21214815). We also thank Prof. Kathy Lui for the generous gift of U6 primer for the qRT-PCR experiment.

■ REFERENCES

(1) Song, S. P.; Qin, Y.; He, Y.; Huang, Q.; Fan, C. H.; Chen, H. Y. Functional Nanoprobes for Ultrasensitive Detection of Biomolecules. *Chem. Soc. Rev.* **2010**, *39*, 4234−4243.

(2) Sato, T.; Takayanagi, A.; Nagao, K.; Tomatsu, N.; Fukui, T.; Kawaguchi, M.; Kudoh, J.; Amagai, M.; Yamamoto, N.; Shimizu, N. Simple PCR-Based DNA Microarray System to Identify Human Pathogenic Fungi in Skin. *J. Clin. Microbiol.* **2010**, *48*, 2357−2364.

(3) Hsieh, K. W.; Patterson, A. S.; Ferguson, B. S.; Plaxco, K. W.; Soh, H. T. Rapid, Sensitive, and Quantitative Detection of Pathogenic DNA at the Point of Care through Microfluidic Electrochemical Quantitative Loop-Mediated Isothermal Amplification. *Angew. Chem., Int. Ed.* **2012**, *51*, 4896−4900.

(4) Wang, C. G.; Xiao, R.; Dong, P. T.; Wu, X. Z.; Rong, Z.; Xin, L.; Tang, J.; Wang, S. Q. Ultra-Sensitive, High-Throughput Detection of Infectious Diarrheal Diseases by Portable Chemiluminescence Imaging. *Biosens. Bioelectron.* **2014**, *57*, 36−40.

(5) Griffin, H. R.; Pyle, A.; Blakely, E. L.; Alston, C. L.; Duff, J.; Hudson, G.; Horvath, R.; Wilson, I. J.; Santibanez-Koref, M.; Taylor, R. W.; Chinnery, P. F. Accurate Mitochondrial DNA Sequencing Using Off-Target Reads Provides a Single Test to Identify Pathogenic Point Mutations. *Genet. Med.* **2014**, *16*, 962−971.

(6) Li, Y., St; John, M. A. R.; Zhou, X. F.; Kim, Y.; Sinha, U.; Jordan, R. C. K.; Eisele, D.; Abemayor, E.; Elashoff, D.; Park, N. H.; Wong, D. T. Salivary Transcriptome Diagnostics for Oral Cancer Detection. *Clin. Cancer Res.* **2004**, *10*, 8442−8450.

(7) Wei, F.; Lillehoj, P. B.; Ho, C. M. DNA Diagnostics: Nanotechnology-Enhanced Electrochemical Detection of Nucleic Acids. *Pediatr. Res.* **2010**, *67*, 458−468.

(8) Reynolds, R. A.; Mirkin, C. A.; Letsinger, R. L. Homogeneous, Nanoparticle-Based Quantitative Colorimetric Detection of Oligonucleotides. *J. Am. Chem. Soc.* **2000**, *122*, 3795−3796.

(9) Fang, Y. M.; Song, J.; Chen, J. S.; Li, S. B.; Zhang, L.; Chen, G. N.; Sun, J. J. Gold Nanoparticles for Highly Sensitive and Selective

DOI: 10.1021/acsami.5b05018
ACS Appl. Mater. Interfaces 2015, 7, 22821−22830

Copper Ions Sensing-Old Materials with New Tricks. *J. Mater. Chem.* **2011**, *21*, 7898−7900.
(10) Eck, D.; Helm, C. A.; Wagner, N. J.; Vaynberg, K. A. Plasmon Resonance Measurements of the Adsorption and Adsorption Kinetics of a Biopolymer onto Gold Nanocolloids. *Langmuir* **2001**, *17*, 957−960.
(11) Englebienne, P. Use of Colloidal Gold Surface Plasmon Resonance Peak Shift to Infer Affinity Constants from the Interactions between Protein Antigens and Antibodies Specific for Single or Multiple Epitopes. *Analyst* **1998**, *123*, 1599−1603.
(12) Kalluri, J. R.; Arbneshi, T.; Afrin Khan, S.; Neely, A.; Candice, P.; Varisli, B.; Washington, M.; McAfee, S.; Robinson, B.; Banerjee, S.; Singh, A. K.; Senapati, D.; Ray, P. C. Use of Gold Nanoparticles in a Simple Colorimetric and Ultrasensitive Dynamic Light Scattering Assay: Selective Detection of Arsenic in Groundwater. *Angew. Chem., Int. Ed.* **2009**, *48*, 9668−9671.
(13) Zhang, M.; Liu, Y. Q.; Ye, B. C. Rapid and Sensitive Colorimetric Visualization of Phthalates Using UTP-Modified Gold Nanoparticles Cross-Linked by Copper(II). *Chem. Commun.* **2011**, *47*, 11849−11851.
(14) Xia, F.; Zuo, X. L.; Yang, R. Q.; Xiao, Y.; Kang, D.; Vallée-Bélisle, A.; Gong, X.; Yuen, J. D.; Hsu, B. B. Y.; Heeger, A. J.; Plaxco, K. W. Colorimetric Detection of DNA, Small Molecules, Proteins, and Ions Using Unmodified Gold Nanoparticles and Conjugated Polyelectrolytes. *Proc. Natl. Acad. Sci. U. S. A.* **2010**, *107*, 10837−10841.
(15) Lou, T. T.; Chen, L. X.; Chen, Z. P.; Wang, Y. Q.; Chen, L.; Li, J. H. Colorimetric Detection of Trace Copper Ions Based on Catalytic Leaching of Silver-Coated Gold Nanoparticles. *ACS Appl. Mater. Interfaces* **2011**, *3*, 4215−4220.
(16) Song, Y. J.; Qu, K. G.; Zhao, C.; Ren, J. S.; Qu, X. G. Graphene Oxide: Intrinsic Peroxidase Catalytic Activity and Its Application to Glucose Detection. *Adv. Mater.* **2010**, *22*, 2206−2210.
(17) Elghanian, R.; Storhoff, J. J.; Mucic, R. C.; Letsinger, R. L.; Mirkin, C. A. Selective Colorimetric Detection of Polynucleotides based on the Distance-Dependent Optical Properties of Gold Nanoparticles. *Science* **1997**, *277*, 1078−1081.
(18) Zhan, Z.; Cao, C.; Sim, S. J. Quantitative Detection of DNA by Autocatalytic Enlargement of Hybridized Gold Nanoprobes. *Biosens. Bioelectron.* **2010**, *26*, 511−516.
(19) Cao, C.; Li, X.; Lee, J.; Sim, S. J. Homogenous Growth of Gold Nanocrystals for Quantification of PSA Protein Biomarker. *Biosens. Bioelectron.* **2009**, *24*, 1292−1297.
(20) Taton, T. A.; Mirkin, C. A.; Letsinger, R. L. Scanometric DNA Array Detection with Nanoparticle Probes. *Science* **2000**, *289*, 1757−1760.
(21) Xu, X. Y.; Georganopoulou, D. G.; Hill, H. D.; Mirkin, C. A. Homogeneous Detection of Nucleic Acids Based Upon the Light Scattering Properties of Silver-Coated Nanoparticle Probes. *Anal. Chem.* **2007**, *79*, 6650−6654.
(22) Li, Y. Y.; Schluesener, H. J.; Xu, S. Q. Gold Nanoparticle-Based Biosensors. *Gold Bull.* **2010**, *43*, 29−41.
(23) Yuan, Z. Q.; Cheng, J.; Cheng, X. D.; He, Y.; Yeung, E. S. Highly Sensitive DNA Hybridization Detection with Single Nanoparticle Flash-Lamp Darkfield Microscopy. *Analyst* **2012**, *137*, 2930−2932.
(24) Kanjanawarut, R.; Su, X. D. Colorimetric Detection of DNA Using Unmodified Metallic Nanoparticles and Peptide Nucleic Acid Probes. *Anal. Chem.* **2009**, *81*, 6122−6129.
(25) Wei, F.; Lam, R.; Cheng, S.; Lu, S.; Ho, D.; Li, N. Rapid Detection of Melamine in Whole Milk Mediated by Unmodified Gold Nanoparticles. *Appl. Phys. Lett.* **2010**, *96*, 133702.
(26) Rastogi, S. K.; Gibson, C. M.; Branen, J. R.; Aston, D. E.; Branen, A. L.; Hrdlicka, P. J. DNA Detection on Lateral Flow Test Strips: Enhanced Signal Sensitivity Using LNA-Conjugated Gold Nanoparticles. *Chem. Commun.* **2012**, *48*, 7714−7716.
(27) Gao, X. F.; Xu, H.; Baloda, M.; Gurung, A. S.; Xu, L. P.; Wang, T.; Zhang, X. J.; Liu, G. D. Visual Detection of MicroRNA with Lateral Flow Nucleic Acid Biosensor. *Biosens. Bioelectron.* **2014**, *54*, 578−584.
(28) Liu, Y. Z.; Wu, Z. T.; Zhou, G. H.; He, Z. K.; Zhou, X. D.; Shen, A. G.; Hu, J. M. Simple, Rapid, Homogeneous Oligonucleotides Colorimetric Detection Based on Non-Aggregated Gold Nanoparticles. *Chem. Commun.* **2012**, *48*, 3164−3166.
(29) Zhou, H.; Kim, J.; Zou, F.; Koh, K.; Park, J.; Lee, J. Rapid Detection of DNA by Magnetophoretic Assay. *Sens. Actuators, B* **2014**, *198*, 77−81.
(30) Baptista, P.; Pereira, E.; Eaton, P.; Doria, G.; Miranda, A.; Gomes, I.; Quaresma, P.; Franco, R. Gold Nanoparticles for the Development of Clinical Diagnosis Methods. *Anal. Bioanal. Chem.* **2008**, *391*, 943−950.
(31) Li, J.; Fu, H. E.; Wu, L. J.; Zheng, A. X.; Chen, G. N.; Yang, H. H. General Colorimetric Detection of Proteins and Small Molecules Based on Cyclic Enzymatic Signal Amplification and Hairpin Aptamer Probe. *Anal. Chem.* **2012**, *84*, 5309−5315.
(32) Zhou, W. J.; Gong, X.; Xiang, Y.; Yuan, R.; Chai, Y. Q. Quadratic Recycling Amplification for Label-Free and Sensitive Visual Detection of HIV DNA. *Biosens. Bioelectron.* **2014**, *55*, 220−224.
(33) Kato, D.; Oishi, M. Ultrasensitive Detection of DNA and RNA Based on Enzyme-Free Click Chemical Ligation Chain Reaction on Dispersed Gold Nanoparticles. *ACS Nano* **2014**, *8*, 9988−9997.
(34) Nam, J. M.; Stoeva, S. I.; Mirkin, C. A. Bio-Bar-Code-Based DNA Detection with PCR-Like Sensitivity. *J. Am. Chem. Soc.* **2004**, *126*, 5932−5933.
(35) Nam, J. M.; Park, S. J.; Mirkin, C. A. Bio-Barcodes Based on Oligonucleotide-Modified Nanoparticles. *J. Am. Chem. Soc.* **2002**, *124*, 3820−3821.
(36) Lee, H.; Park, J. E.; Nam, J. M. Bio-Barcode Gel Assay for MicroRNA. *Nat. Commun.* **2014**, *5*, 3367.
(37) Liao, Y. H.; Huang, R.; Ma, Z. K.; Wu, Y. X.; Zhou, X. M.; Xing, D. Target-Triggered Enzyme-Free Amplification Strategy for Sensitive Detection of MicroRNA in Tumor Cells and Tissues. *Anal. Chem.* **2014**, *86*, 4596−4604.
(38) Liu, P.; Yang, X. H.; Sun, S.; Wang, Q.; Wang, K. M.; Huang, J.; Liu, J. B.; He, L. L. Enzyme-Free Colorimetric Detection of DNA by Using Gold Nanoparticles and Hybridization Chain Reaction Amplification. *Anal. Chem.* **2013**, *85*, 7689−7695.
(39) Quan, K.; Huang, J.; Yang, X. H.; Yang, Y. J.; Ying, L.; Wang, H.; He, Y.; Wang, K. M. An Enzyme-Free and Amplified Colorimetric Detection Strategy via Target-Aptamer Binding Triggered Catalyzed Hairpin Assembly. *Chem. Commun.* **2015**, *51*, 937−940.
(40) Quan, K.; Huang, J.; Yang, X. H.; Yang, Y. J.; Ying, L.; Wang, H.; Wang, K. M. An Enzyme-Free and Amplified Colorimetric Detection Strategy: Assembly Of Gold Nanoparticles Through Target-Catalytic Circuits. *Analyst* **2015**, *140*, 1004−1007.
(41) Xuan, F.; Hsing, I. M. Triggering Hairpin-Free Chain-Branching Growth of Fluorescent DNA Dendrimers for Nonlinear Hybridization Chain Reaction. *J. Am. Chem. Soc.* **2014**, *136*, 9810−9813.
(42) Ma, C. P.; Wu, Z. W.; Wang, W. S.; Jiang, Q. Q.; Shi, C. Three-dimensional DNA Nanostructures for Colorimetric Assay of Nucleic Acids. *J. Mater. Chem. B* **2015**, *3*, 2853−2857.
(43) Hurst, S. J.; Lytton-Jean, A. K. R.; Mirkin, C. A. Maximizing DNA Loading on a Range of Gold Nanoparticle Sizes. *Anal. Chem.* **2006**, *78*, 8313−8318.
(44) Song, J. Y.; Lee, C. H.; Choi, E. J.; Kim, K.; Yoon, J. Y. Sensitive Mie Scattering Immunoagglutination Assay of Porcine Reproductive and Respiratory Syndrome Virus (PRRSV) from Lung Tissue Samples in a Microfluidic Chip. *J. Virol. Methods* **2011**, *178*, 31−38.
(45) Ma, C. P.; Wang, W. S.; Li, Z. X.; Cao, L. J.; Wang, Q. Y. Simple Colorimetric DNA Detection Based on Hairpin Assembly Reaction and Target-Catalytic Circuits for Signal Amplification. *Anal. Biochem.* **2012**, *429*, 99−102.
(46) Mitchell, P. S.; Parkin, R. K.; Kroh, E. M.; Fritz, B. R.; Wyman, S. K.; Pogosova-Agadjanyan, E. L.; Peterson, A.; Noteboom, J.; O'Briant, K. C.; Allen, A.; Lin, D. W.; Urban, N.; Drescher, C. W.; Knudsen, B. S.; Stirewalt, D. L.; Gentleman, R.; Vessella, R. L.; Nelson, P. S.; Martin, D. B.; Tewari, M. Circulating MicroRNAs as Stable Blood-Based Markers for Cancer Detection. *Proc. Natl. Acad. Sci. U. S. A.* **2008**, *105*, 10513−10518.

DOI: 10.1021/acsami.5b05018
ACS Appl. Mater. Interfaces 2015, 7, 22821−22830

(47) Chen, J.; Wang, B. C.; Tang, J. H. Clinical Significance of MicoRNA-155 Expression in Human Breast Cancer. *J. Surg. Oncol.* **2012**, *106*, 260−266.
(48) Jiang, S. A.; Zhang, H. W.; Lu, M. H.; He, X. H.; Li, Y.; Gu, H.; Liu, M. F.; Wang, E. D. MicroRNA-155 Functions as an OncomiR in Breast Cancer by Targeting the Suppressor of Cytokine Signaling 1 Gene. *Cancer Res.* **2010**, *70*, 3119−3127.
(49) Chi, B. Z.; Liang, R. P.; Zhang, L.; Qiu, J. D. Sensitive and Homogeneous MicroRNA Detection Using Branched Cascade Enzymatic Amplification. *Chem. Commun.* **2015**, *51*, 10543−10546.
(50) Wiscombe, W. J. Improved Mie Scattering Algorithms. *Appl. Opt.* **1980**, *19*, 1505−1509.
(51) Ashkin, A.; Dziedzic, J. M.; Bjorkholm, J. E.; Chu, S. Observation of a Single-Beam Gradient Force Optical Trap for Dielectric Particles. *Opt. Lett.* **1986**, *11*, 288−290.
(52) Lechner, M. D. Influence of Mie Scattering on Nanoparticles with Different Particle Sizes and Shapes: Photometry and Analytical Ultracentrifugation with Absorption Optics. *J. Serb. Chem. Soc.* **2005**, *70*, 361−369.
(53) Retsch, M.; Schmelzeisen, M.; Butt, H. J.; Thomas, E. L. Visible Mie Scattering in Nonabsorbing Hollow Sphere Powders. *Nano Lett.* **2011**, *11*, 1389−94.
(54) Xu, H.; Chen, X. Q.; Ouyang, S. X.; Kako, T.; Ye, J. H. Size-Dependent Mie's Scattering Effect on TiO_2 Spheres for the Superior Photoactivity of H_2 Evolution. *J. Phys. Chem. C* **2012**, *116*, 3833−3839.
(55) Liu, X.; Atwater, M.; Wang, J. H.; Huo, Q. Extinction Coefficient of Gold Nanoparticles With Different Sizes and Different Capping Ligands. *Colloids Surf., B* **2007**, *58*, 3−7.

DOI: 10.1021/acsami.5b05018
ACS Appl. Mater. Interfaces 2015, 7, 22821−22830